Inverse energy transfer in three-dimensional quantum vortex flows

P. Z. Stasiak, A. Baggaley, and C.F. Barenghi School of Mathematics, Statistics and Physics, Newcastle University, Newcastle upon Tyne, NE1 7RU, United Kingdom

G. Krstulovic

Université Côte d'Azur, Observatoire de la Côte d'Azur, CNRS, Laboratoire Lagrangre, Boulevard de l'Observatoire CS 34229 - F 06304 NICE Cedex 4, France

L. Galantucci

Istituto per le Applicazioni del Calcolo "M. Picone" IAC CNR, Via dei Taurini 19, 00185 Roma, Italy (Dated: March 5, 2025)

Vortex reconnections play a fundamental role in fluids. They increase the complexity of flow and develop small-scale motions. In this work, we report that in superfluids, they can also excite large scales. We numerically illustrate that during a superfluid vortex reconnection energy is injected into the thermal (normal) component of helium II at small length scales, but is transferred nonlinearly to larger length scales, increasing the integral length scale of the normal fluid. We show that this inverse energy transfer is triggered by the helical imbalance generated in the normal fluid flow by the mutual friction force coupling the superfluid vortices and the normal component. We finally discuss the relevance of our findings to the problem of superfluid turbulence.

Turbulence is ubiquitous in the universe. It occurs in systems as large as nebulae of interstellar gas, and as small as clouds of few thousands atoms confined by lasers in the laboratory. Turbulence shapes patterns and properties of fluids of all kinds, from ordinary viscous fluids (Navier-Stokes turbulence[1]) to electrically conducting fluids (magneto-hydrodynamics turbulence [2]) to quantum fluid (quantum turbulence [3, 4]). All turbulent systems are characterised by the existence of a wide range of length scales across which inviscid conserved quantities are transferred without loss in the spirit of the cascade depicted by Richardson [5].

In three-dimensional (3D) classical fluids, turbulence is characterised by a direct cascade: the non-linear dissipationless transfer of kinetic energy from the scale of the large eddies (at which energy is injected) to the smallest length scales at which energy is dissipated into heat [5, 6]. The resulting distribution of energy across length scales is the celebrated Kolmogorov energy spectrum [1, 6].

Confining Navier-Stokes turbulence to two-dimensions (2D) entails fundamentally distinct physics: a dual cascade emerges of energy and enstrophy (mean squared vorticity) [7, 8], the two conserved quantities in ideal two-dimensional flows. While the enstrophy cascade is direct (from large to small scales), the energy cascade is inverse (from small to large scales) [9]. This inverse cascade may favour the generation and persistence of large coherent structures [10].

Remarkably, the same cascade phenomenology is observed in turbulent flows of quantum fluids, *i.e.* fluids at very low temperatures whose physics is dominated by quantum effects. Examples of such fluids are superfluid helium and atomic Bose-Einstein Condensates (BECs).

The dynamics of these systems can be successfully depicted in terms of a two-fluid model [11–13] describing the quantum fluid as the mixture of two components, the superfluid component and the thermal (or normal) component, which interact by means of a mutual friction force [14–16]. The superfluid component flows without viscosity and vanishing entropy; its vorticity is confined to effectively one-dimensional vortex filaments of atomic core thickness (called quantum vortices or vortex lines), around which the circulation of the velocity is quantised. In BECs the thermal component forms a ballistic gas, whereas in superfluid ⁴He it can be described as a classical viscous fluid. Despite these significant differences with respect to ordinary fluids, the direct kinetic energy cascade has indeed been observed in three-dimensional superfluid turbulence [17– 22. Evidence of this direct cascade has been found also in three-dimensional turbulent BECs [23]. Similarly to 2D classical turbulence, an inverse energy cascade characterises turbulence in two-dimensional BECs, as shown in theoretical [24–27] and experimental [28, 29] studies.

In turbulent systems, the type and the number of sign-defined ideal invariants determine the direction of cascades. Indeed, the famous Fjørtoft argument [30] predicts the existence of an inverse energy cascade in 2D classical turbulence. It also predicts an inverse particle and a direct energy cascade for 3D wave turbulent BECs, as recently addressed theoretically [31]. In 3D classical fluids, helicity, which is also an inviscid invariant, is not sign-defined and thus only a direct energy cascade is possible. However, recent studies have demonstrated that the direction of the energy cascade may be inverted by artificially controlling the chirality of the flow, *i.e.*

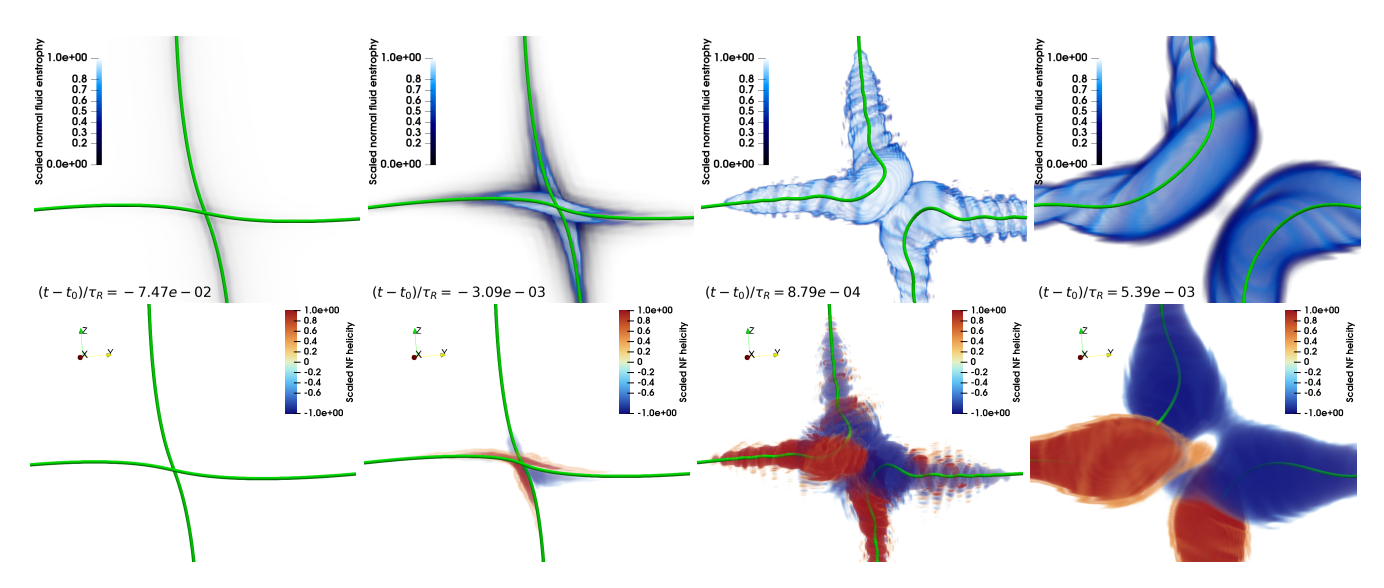


FIG. 1: Three-dimensional rendering of the time evolution of an initially orthogonal vortex configuration undergoing a vortex reconnection at $T=1.9{\rm K}$ at dimensionless times (from left to right) $(t-t_R)/\tau_R=-7.47\times 10^{-2}$, -3.09×10^{-3} , 8.79×10^{-4} and 5.39×10^{-3} , where $\tau_R=E_R^{1/2}/L_R$. The green tubes represent the superfluid vortex lines (the tubes' radii have been greatly exaggerated for visual purpose). In the top sequence, the blue volume rendering represents the scaled normal fluid enstrophy ω^2/ω_{max}^2 . Note the Kelvin wave on the superfluid vortex at $(t-t_0)/\tau_R=8.79\times 10^{-4}$. In the bottom sequence, the red/blue volume rendering at the same times represent scaled positive/negative normal fluid helicity.

the balance between positive and negative helical modes [32]. Indeed, by restricting the non-linear energy transfer to homochiral interactions via a suitable decimation of the Navier-Stokes equation [33, 34], by controlling the weight of homochiral interactions [35], or by the external injection of positive helical modes at all length scales [36], inverse energy cascades have been observed in three-dimensional turbulence of classical fluids. In brief, when the flow is synthetically designed to have an enhanced chirality, an inverse energy cascade can observed.

In this work, we unveil a similar dynamics occurring in superfluid helium (⁴He) as a result of vortex Reconnections occur continuously in reconnections. turbulence: they take place when two vortex lines collide and recombine, exchanging heads and tails, altering the overall topology of the flow [37–43]. We show that the mutual friction force arising from the vortex reconnection is chiral, injecting in the normal fluid prevalently helicity of a given sign. Thus, as a consequence of vortex reconnections, we observe an increase of the chiral imbalance of the quantum fluid, producing a transfer of kinetic energy from small to large scales, similarly to the phenomenology observed in 3D helical-decimated Unlike classical fluids, such a chiral classical flows. imbalance arises naturally as physical process in the normal fluid.

To model superfluid helium dynamics, we employ the recently developed FOUCAULT model [44]. In this approach, superfluid vortex lines are parametrized as one-dimensional space curves $\mathbf{s}(\xi,t)$, ξ and t being arclength and time respectively, exploiting the large separation of length scales between the vortex core radius, the Lagrangian discretisation along the vortex lines $\Delta \xi$, and the average radius of curvature R_c of the vortex lines. The vortex lines evolve according to the following equation of motion:

$$\dot{\mathbf{s}}(\xi, t) = \mathbf{v}_s + \frac{\beta}{1+\beta} \left[\mathbf{v}_{ns} \cdot \mathbf{s}' \right] \mathbf{s}' + \beta \mathbf{s}' \times \mathbf{v}_{ns} + \beta' \mathbf{s}' \times \left[\mathbf{s}' \times \mathbf{v}_{ns} \right],$$
(1)

where $\dot{\mathbf{s}} = \partial \mathbf{s}/\partial t$, $\mathbf{s}' = \partial \mathbf{s}/\partial \xi$ is the unit tangent vector, \mathbf{v}_n and \mathbf{v}_s are the normal fluid and superfluid velocities at \mathbf{s} , $\mathbf{v}_{ns} = \mathbf{v}_n - \mathbf{v}_s$, and β , β' are temperature and Reynolds number dependent mutual friction coefficients [44]. The calculation of the superfluid velocity \mathbf{v}_s is performed via the computation of the Biot-Savart integral de-singularised with standard techniques (see Supplementary Material [45]). The normal fluid is described classically using the incompressible $(\nabla \cdot \mathbf{v}_n = 0)$ Navier-Stokes equation

$$\frac{\partial \mathbf{v}_n}{\partial t} + (\mathbf{v}_n \cdot \nabla) \mathbf{v}_n = -\frac{1}{\rho} \nabla p + \nu_n \nabla^2 \mathbf{v}_n + \frac{\mathbf{F}_{ns}}{\rho_n} , \quad (2)$$

where ρ_n and ρ_s are the normal fluid and superfluid densities, $\rho = \rho_n + \rho_s$, p is the pressure, ν_n is the kinematic viscosity of the normal fluid, and the mutual friction force per unit volume, \mathbf{F}_{ns} , is the line integral of

the mutual friction force per unit length, \mathbf{f}_{ns} [45]:

$$\mathbf{F}_{ns}(\mathbf{x}) = \oint_{\mathcal{C}} \delta(\mathbf{x} - \mathbf{s}) \mathbf{f}_{ns}(\mathbf{s}) d\xi, \qquad (3)$$

 \mathcal{C} representing the entire vortex configuration. The regularisation of mutual friction is performed using a physically self-consistent scheme [44]. We consider a periodical box of size 2π (so that wavevectors are integers).

To study the reconnection dynamics, we consider two pairs of initially orthogonal vortices (where the corresponding vortices of each pair have opposite circulation in order to preserve periodicity along the boundaries) at two distinct temperatures, T=1.9K and T=2.1K. The vortex pairs are separated by the distance D_{ℓ} ; each vortex within each pair is initially at distance d_{ℓ} to the other vortex, such that $d_{\ell} \ll D_{\ell}$ to ensures that the dynamics in the vicinity of the reconnection is dominated by local interactions, and that the far-field contribution from the other vortex pair is negligible.

The evolution of the vortex reconnection of a single pair is reported in Fig. 1. The first row shows the reconnecting superfluid vortices (in green) accompanied by normal fluid structures generated by mutual friction, here displayed as enstrophy rendering $\omega(\mathbf{x})^2 = |\nabla \times \mathbf{v}_n|^2$. Such structures are the signature of the violent irreversible energy transfers in vortex reconnections [46]. The second row shows the rendering of the local helicity $H(\mathbf{x}) = \mathbf{v}_n \cdot \boldsymbol{\omega}$, where we observe a clear local helicity production, with an abrupt change of sign due to the rearrangement of the vortex topology. Remarkably, during reconnection there is a net sudden normal fluid helicity production, as shown in Fig. 2. We will come back to this finding later.

We now focus on the time evolution of the normal fluid energy spectrum E(k), defined by

$$E = \frac{1}{(2\pi)^3} \int_{\mathcal{V}} \frac{1}{2} |\mathbf{v}_n|^2 dV = \int_0^\infty E(k) dk$$
 (4)

where E is the total normal fluid energy and k is the magnitude of the three-dimensional wavenumber. The energy at reconnection E_R is given by $E(t_R)$, where t_R is the time at reconnection. The energy spectrum E(k) is displayed in Fig. 3a.

It clearly emerges that, during the reconnection, energy is predominantly injected into the normal fluid at intermediate and small length scales. For k > 5 in correspondence of the reconnection time t_R , we observe a significant increase of the normal fluid energy spectral density: $E(k, t \approx t_R)/E(k, t \ll t_R) \approx 10^2$. In the post-reconnection regime, we simultaneously observe a small decrease of the spectrum at intermediate and small scales (k > 5) and an increase at large scales, suggesting the existence of a mechanism by which energy generated at

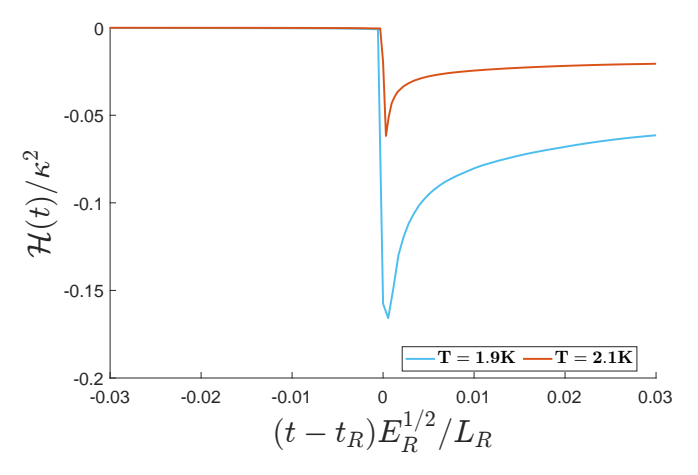


FIG. 2: Temporal evolution of the normal fluid helicity $\mathcal{H} = \int_{\mathcal{V}} H(\mathbf{x}) dV$ computed over the entire volume \mathcal{V} . For superfluid helium, it is proper to make the helicity dimensionless in terms of κ^2 . The quantities E_R and L_R are the energy E and integral length scales L_0 of the normal fluid at reconnection time t_R .

small length scales is transferred to larger scales. To shed light on this mechanism, as customary for turbulent flows, we analyse the spectral energy flux

$$\Pi(k) = \int_{|\mathbf{p}| \le k} \hat{\mathbf{v}}_n^* \cdot \left[(\widehat{\mathbf{v}_n \cdot \nabla}) \mathbf{v}_n \right] d\mathbf{p} + c.c. , \quad (5)$$

where $\hat{\cdot}$ indicates the Fourier transform.

We observe that $\Pi(k) < 0$ for all k during and after reconnection; we also observe that, near the time of reconnection, the peak value of $|\Pi(k)|$ is in the range 15 < k < 25. The negative sign of $\Pi(k)$ is evidence of a flux of kinetic energy from small to large scales, exciting larger and larger scales. This behaviour is quantified by the evolution of the integral length scale L_0 , defined as

$$L_0 = \frac{\pi}{2E} \int_0^\infty \frac{E(k)}{k} dk,\tag{6}$$

The inset of Fig. 3b shows that L_0 indeed increases steadily in the post-reconnection regime. Note that times have been normalised by the largest eddy-turnover-time at the reconnection event, evidencing it fast evolution.

To explain the inverse energy transfer shown in Fig. 3a, we look whether the reconnection triggers a chirality imbalance. We decompose the incompressible Fourier modes of the normal fluid velocity into helical modes [47]:

$$\hat{\mathbf{v}}_n(\mathbf{k}) = \hat{\mathbf{v}}_n^+(\mathbf{k}) + \hat{\mathbf{v}}_n^-(\mathbf{k}) = v_n^+(\mathbf{k})\mathbf{h}^+(\mathbf{k}) + v_n^-(\mathbf{k})\mathbf{h}^-(\mathbf{k}),$$
(7)

where $\mathbf{h}^{\pm}(\mathbf{k})$ are the two eigenvectors of the curl operator, *i.e.* $i\mathbf{k} \times \mathbf{h}^{\pm}(\mathbf{k}) = \pm k\mathbf{h}^{\pm}(\mathbf{k})$. Similarly, we decompose the transverse modes of the mutual friction force: $\hat{\mathbf{F}}_{ns}^{\perp}(\mathbf{k}) = f^{+}(\mathbf{k})\mathbf{h}^{+} + f^{-}(\mathbf{k})\mathbf{h}^{-}$ (the Fourier modes of \mathbf{F}_{ns} parallel to the wavenumber \mathbf{k} do not play any

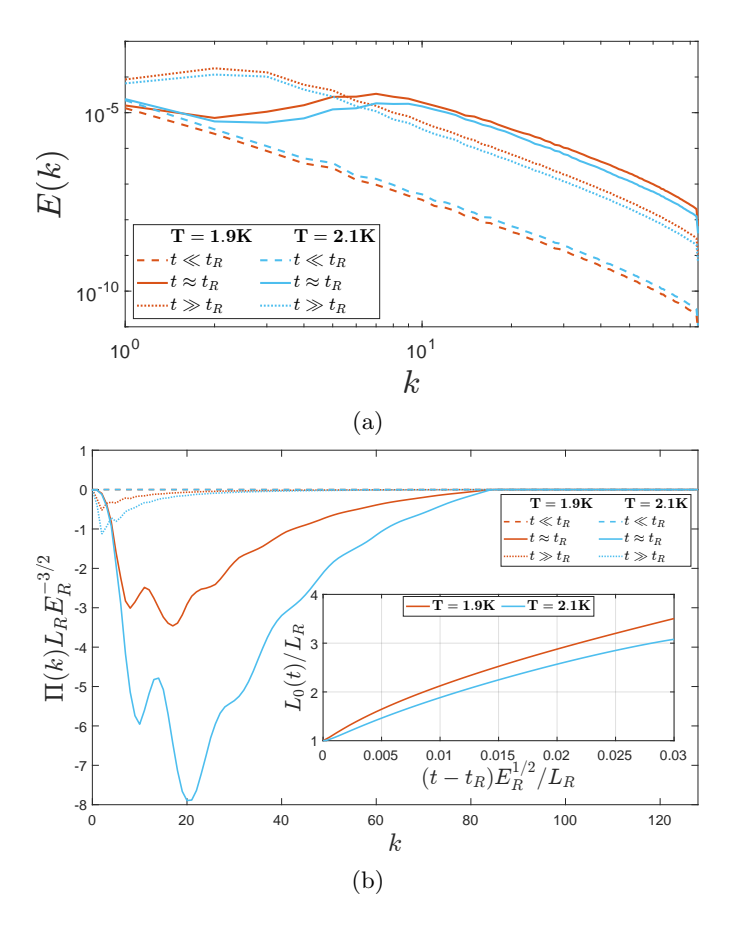


FIG. 3: (a): Normal fluid kinetic energy spectrum E(k) before reconnection (dashed lines), at reconnection (solid lines) and after reconnection (dotted lines) for T = 1.9K (red) and T = 2.1K (blue).(b): Spectral normal fluid kinetic energy flux, $\Pi(k)$. It is normalised using the integral scale and the normal fluid energy at reconnection. Inset: Post reconnection evolution of the integral length scale, L_0 . Times and temperatures are labelled as in Fig. 3a.

role in the time evolution of \mathbf{v}_n due to the incompressible constraint). Finally, the helical decomposition naturally allow us decompose the total helicity as $\mathcal{H} = \mathcal{H}^+ - \mathcal{H}^-$ [36].

A chiral imbalance occurs if the mutual friction force is helical, i.e. if the ratio $|f^+|^2/|f^-|^2 \neq 1$, with $|f^{\pm}|^2$ the total squared norm of the mutual friction components. In Fig. 4, we show the temporal evolution of $|f^+|^2/|f^-|^2$, for both temperatures. It is apparent that during and after the reconnection, the mutual friction force is strongly chiral, injecting more negative helicity than positive helicity. As a result, the ratio $\mathcal{H}^+/\mathcal{H}^-$ (reported in the inset of Fig. 4) decreases significantly at reconnection and remains smaller than unity even at later times, indicating that the flow is persistently chiral. We conclude that the reconnection triggers indeed a chiral imbalance. From Fig. 4 we determine the non-

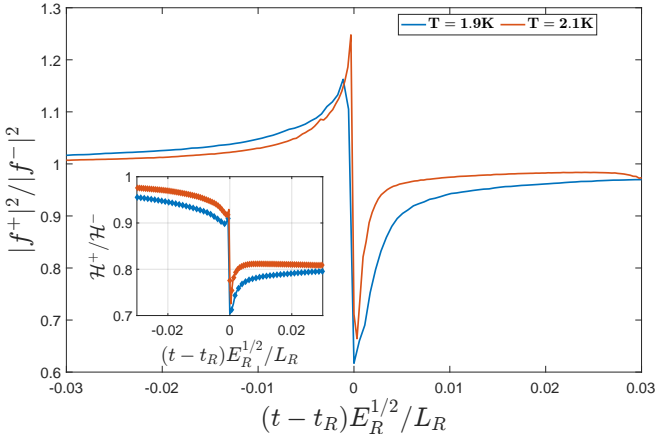


FIG. 4: Temporal evolution of projected mutual friction force components $f^{\pm}/$ Inset: temporal evolution of total helical components.

dimensional timescale $\tau=(t^*-t_R)E_R^{1/2}/L_R$ during which the mutual friction force is chiral as a result of reconnections: $\tau\approx 0.01$ and $\tau\approx 0.005$ for $T=1.9{\rm K}$ and $T=2.1{\rm K}$, respectively, corresponding dimensionally to $\tau\approx 0.1{\rm s}$ for both temperatures. In superfluid turbulence, the timescale between two consecutive reconnections can be smaller than τ provided that the vortex line density $\mathcal L$ (length of vortices per unit volume) is larger than $10^8{\rm m}^{-2}$ [46, 48], a condition which is easily met in superfluid helium experiments [49, 50].

In conclusion, the reconnection of quantum vortices in the two-fluid regime $(T\gtrsim 1.5\mathrm{K})$ not only injects punctuated energy in the normal fluid [46], but also triggers in the normal fluid a transfer of kinetic energy towards the large scales. This inverse energy transfer arises from the helical character of the friction generated by the Kelvin waves released by the reconnecting cusp, which produces a chiral imbalance in the normal fluid, as previously observed in turbulent Navier-Stokes flows [33, 36].

Our findings have profound implications for the nature of turbulence in finite temperature superfluids. circumstances where the vortex density \mathcal{L} is large and where the isotropy of the vortex tangle is broken by external forcing, the chirality of the flow generated by the frequent reconnections may be strong enough to induce an inverse energy cascade [51]. The microscopic mechanism that we have described is probably what triggers the inverse energy cascade which is observed numerically in large-scale simulations of counterflow turbulence at large heat fluxes [52], which indeed inherently not isotropic. Our work hence motivates further detailed studies of the role played by helicity in superfluid dynamics [53, 54], moving the emphasis from few vortex systems [55] to fully coupled superfluid turbulence.

G.K. was supported by the Agence Nationale de la Recherche through the project the project QuantumVIW ANR-23-CE30-0024-02. This work has been also supported by the French government, through the UCAJEDI Investments in the Future project managed by the National Research Agency (ANR) with the reference number ANR-15-IDEX-01. P.Z.S. acknowledges the financial support of the UniCA "visiting doctoral student program" on complex systems. Computations were carried out at the Mésocentre SIGAMM hosted at the Observatoire de la Côte d'Azur.

- [1] U. Frisch, Turbulence: The Legacy of A. N. Kolmogorov (1995).
- [2] V. M. Canuto and J. Christensen-Dalsgaard, Turbulence in astrophysics: stars, Ann. Rev. Fluid Mech. 30, 167 (1998).
- [3] C. F. Barenghi, H. A. J. Middleton-Spencer, L. Galantucci, and N. G. Parker, Types of quantum turbulence, AVS Quantum Sci. 5, 025601 (2023).
- [4] C. F. Barenghi, L. Skrbek, and K. R. Sreenivasan, Quantum Turbulence (Cambridge University Press, 2023).
- [5] L. F. Richardson, Weather Prediction by Numerical Process (University Press, 1922).
- [6] A. Kolmogorov, The local structure of turbulence in an incompressible viscous fluid for very large Reynolds numbers, Dokl. Akad. Nauk. SSSR 30, 301 (1941).
- [7] R. Kraichnan, Inertial ranges in two-dimensional turbulence, Phys. Fluids **10**, 1417 (1967).
- [8] G. Boffetta and R. E. Ecke, Two-dimensional turbulence, Ann. Rev. Fluid Mech. 44, 427 (2012).
- [9] G. Boffetta and S. Musacchio, Evidence for the double cascade scenario in two-dimensional turbulence, Phys. Rev. E 82, 016307 (2010).
- [10] J. Laurie, G. Boffetta, G. Falkovich, I. Kolokolov, and V. Lebedev, Universal profile of the vortex condensate in two-dimensional turbulence, Phys. Rev. Lett. 113, 254503 (2014).
- [11] L. Tisza, Transport phenomena in helium II, Nature 141, 913 (1938).
- [12] L. Landau, On the theory of superfluidity, Phys. Rev. 75, 884 (1949).
- [13] L. Skrbek and K. R. Sreenivasan, Developed quantum turbulence and its decay, Phys. Fluids 24, 011301 (2012).
- [14] B. Jackson, N. P. Proukakis, C. F. Barenghi, and E. Zaremba, Finite-temperature vortex dynamics in boseeinstein condensates, Phys. Rev. A 79, 053615 (2009).
- [15] H. E. Hall and W. F. Vinen, The rotation of liquid helium II. i. experiments on the propagation of secound sound in uniformly rotating helium II, Proc. R. Soc. London A 238, 204 (1956).
- [16] H. E. Hall and W. F. Vinen, The rotation of liquid helium II. ii. the theory of mutual friction in uniformly rotating helium II, Proc. R. Soc. London A 238, 215 (1956).
- [17] J. Maurer and P. Tabeling, Local investigation of superfluid turbulence, Europhys. Lett. 43, 29 (1998).
- [18] J. Salort, C. Baudet, B. Castaing, B. Chabaud,

- F. Daviaud, T. Didelot, P. Diribarne, B. Dubrulle, Y. Gagne, F. Gauthier, A. Girard, B. Hébral, R. B., P. Thibault, and P.-E. Roche, Turbulent velocity spectra in superfluid flows, Phys. Fluids **22** (2010).
- [19] A. W. Baggaley, L. K. Sherwin, C. F. Barenghi, and Y. A. Sergeev, Thermally and mechanically driven quantum turbulence in helium II, Phys. Rev. B 86, 104501 (2012).
- [20] L. K. Sherwin-Robson, C. F. Barenghi, and A. W. Baggaley, Local and nonlocal dynamics in superfluid turbulence, Phys. Rev. B 91, 104517 (2015).
- [21] N. P. Müller and G. Krstulovic, Kolmogorov and Kelvin wave cascades in a generalized model for quantum turbulence, Phys, Rev. B 102, 134513 (2020).
- [22] N. P. Müller, J. I. Polanco, and G. Krstulovic, Intermittency of Velocity Circulation in Quantum Turbulence, Phys, Rev. X 11, 011053 (2021).
- [23] H. A. J. Middleton-Spencer, A. D. G. Orozco, L. Galantucci, M. Moreno, N. G. Parker, L. A. Machado, V. S. Bagnato, and C. F. Barenghi, Evidence of strong quantum turbulence in Bose-Einstein condensates, Phys. Rev. Research 5, 043081 (2022).
- [24] A. S. Bradley and B. P. Anderson, Energy spectra of vortex distributions in two-dimensional quantum turbulence, Phys. Rev. X 2, 041001 (2012).
- [25] M. T. Reeves, T. P. Billam, B. P. Anderson, and A. S. Bradley, Inverse energy cascade in forced twodimensional quantum turbulence, Phys. Rev. Lett. 110, 104501 (2013).
- [26] T. Simula, M. J. Davis, and K. Helmerson, Emergence of order from turbulence in an isolated planar superfluid, Phys. Rev. Lett. 113, 165302 (2014).
- [27] N. P. Müller and G. Krstulovic, Exploring the Equivalence between Two-Dimensional Classical and Quantum Turbulence through Velocity Circulation Statistics, Phys, Rev. Letters 132, 094002 (2024).
- [28] S. P. Johnstone, A. J. Groszek, P. T. Starkey, C. J. Billington, T. P. Simula, and K. Helmerson, Evolution of large-scale flow from turbulence in a two-dimensional superfluid, Science 364, 1267 (2019).
- [29] G. Gauthier, M. T. Reeves, X. Yu, A. S. Bradley, M. A. Baker, T. A. Bell, H. Rubinsztein-Dunlop, M. J. Davis, and T. W. Neely, Giant vortex clusters in a twodimensional quantum fluid, Science 364, 1264 (2019).
- [30] R. Fjørtoft, On the changes in the spectral distribution of kinetic energy for twodimensional, nondivergent flow, Tellus 5, 225 (1953).
- [31] Y. Zhu, B. Semisalov, G. Krstulovic, and S. Nazarenko, Direct and Inverse Cascades in Turbulent Bose-Einstein Condensates, Phys, Rev. Letters 130, 133001 (2023).
- [32] H. K. Moffatt, The degree of knottedness of tangled vortex lines, J. Fluid Mech. **36**, 7 (1969).
- [33] L. Biferale, S. Musacchio, and F. Toschi, Inverse energy cascade in three-dimensional isotropic turbulence, Phys. Rev. Lett. 108, 164501 (2012).
- [34] L. Biferale, S. Musacchio, and F. Toschi, Split energy-helicity cascades in three-dimensional homogeneous and isotropic turbulence, J. Fluid Mech. 730, 309–327 (2013).
- [35] G. Sahoo, A. Alexakis, and L. Biferale, Discontinuous transition from direct to inverse cascade in threedimensional turbulence, Phys. Rev. Lett. 118, 164501 (2017).
- [36] F. Plunian, A. Teimurazov, R. Stepanov, and M. K. Verma, Inverse cascade of energy in helical turbulence,

- J. Fluid Mech. 895, A13 (2020).
- [37] J. Koplik and H. Levine, Vortex reconnection in superfluid helium, Phys. Rev. Lett. 71, 1375 (1993).
- [38] G. P. Bewley, M. S. Paoletti, K. R. Sreenivasan, and D. P. Lathrop, Characterization of reconnecting vortices in superfluid helium, Proc. Natl. Acad. Sci. USA 105, 13707 (2008).
- [39] C. Rorai, J. Skipper, R. Kerr, and K. Sreenivasan, Approach and separation of quantum vortices with balanced cores, J. Fluid Mech. 808, 641 (2016).
- [40] S. Serafini, L. Galantucci, E. Iseni, T. Bienaime, R. Bisset, C. F. Barenghi, F. Dalfovo, G. Lamporesi, and G. Ferrari, Vortex reconnections and rebounds in trapped atomic Bose-Einstein condensates, Phys. Rev. X 7, 021031 (2017).
- [41] L. Galantucci, A. W. Baggaley, N. G. Parker, and C. F. Barenghi, Crossover from interaction to driven regimes in quantum vortex reconnections, Proc. Natl. Acad. Sci. USA 116, 12204 (2019).
- [42] A. Villois, D. Proment, and G. Krstulovic, Universal and nonuniversal aspects of vortex reconnections in superfluids, Phys, Rev. Fluids 2, 044701 (2017).
- [43] A. Villois, D. Proment, and G. Krstulovic, Irreversible dynamics of vortex reconnections in quantum fluids, Phys. Rev. Lett. 125, 164501 (2020).
- [44] L. Galantucci, A. W. Baggaley, C. F. Barenghi, and G. Krstulovic, A new self-consistent approach of quantum turbulence in superfluid helium, Eur. Phys. J. Plus 135, 547 (2020).
- [45] See supplementary materials.
- [46] P. Z. Stasiak, Y. Xing, Y. Alihosseini, C. F. Barenghi, A. W. Baggaley, W. Guo, L. Galantucci, and G. Krstulovic, Experimental and theoretical evidence of universality in superfluid vortex reconnections, arXiv, 2411.08942 (2024).
- [47] F. Waleffe, The nature of triad interactions in homogeneous turbulence, Phys. Fluids A 4, 350 (1992).
- [48] C. F. Barenghi and D. C. Samuels, Scaling laws of vortex reconnections, J. Low Temp. Phys. 136, 281 (2004).
- [49] P.-E. Roche, P. Diribarne, T. Didelot, O. Français, L. Rousseau, and H. Willaime, Vortex density spectrum of quantum turbulence, EPL 77, 66002 (2007).
- [50] S. Babuin, E. Varga, L. Skrbek, E. Lévêque, and P.-E. Roche, Effective viscosity in quantum turbulence: a steady state approach, Europhys. Lett. 106, 24006 (2014).
- [51] The symmetry breaking of the vortex configuration is a key element, as perfectly symmetrical reconnections (with opposite vortex line orientations) would inject net helicities of opposite sign leading globally to a non-chiral flow
- [52] J. Polanco and G. Krstulovic, Counterflow-induced inverse energy cascade in three-dimensional superfluid turbulence, Phys. Rev. Lett. 125, 254504 (2020).
- [53] P. Di Leoni, P. Mininni, and B. ME, Dual cascade and dissipation mechanisms in helical quantum turbulence, Phys. Rev. A 95, 053636 (2026).
- [54] L. Galantucci, CF. Barenghi, NG. Parker, and AW. Baggaley, Mesoscale helicity distinguishes Vinen from Kolmogorov turbulence in helium-II, Phys. Rev. B 103, 144503 (2021).
- [55] M. Scheeler, D. Kleckner, D. Proment, G. Kindlmann, and I. WTM, Helicity conservation by flow across scales in reconnecting vortex links and knots, Proc Natl Acad

- Sci Usa 111, 15350 (2014).
- [56] KW. Schwarz, Three-dimensional vortex dynamics in superfluid ⁴He, Phys. Rev. B 38, 2398 (1988).
- [57] D. Proment and G. Krstulovic, Matching theory to characterize sound emission during vortex reconnection in quantum fluids, Phys. Rev. Fluids 5, 104701 (2020).
- [58] A. W. Baggaley, The sensitivity of the vortex filament method to different reconnection models, J. Low Temp. Phys. 168, 18 (2012).
- [59] L. Galantucci, M. Sciacca, and CF. Barenghi, Coupled normal fluid and superfluid profiles of turbulent helium II in channels, Phys Rev B 92, 174530 (2015).
- [60] P. Gualtieri, F. Picano, G. Sardina, and C. M. Casciola, Exact regularized point particle method for multiphase flows in the two-way coupling regime, J. Fluid Mech. 773, 520 (2015).
- [61] P. Gualtieri, F. Battista, and C. M. Casciola, Turbulence modulation in heavy-loaded suspensions of tiny particles, Phys. Rev. Fluids 2, 034304 (2017).

SUPPLEMENTARY MATERIALS

Using Schwarz mesoscopic model [56], vortex lines can be described as space curves $\mathbf{s}(\xi,t)$ of infinitesimal thickness, with a single quantum of circulation $\kappa = h/m_4 = 9.97 \times 10^{-8} \mathrm{m}^2/\mathrm{s}$, where h is Planck's constant, $m_4 = 6.65 \times 10^{-27} \mathrm{kg}$ is the mass of one helium atom, ξ is the natural parameterisation, arclength, and t is time. These conditions are a good approximation, since the vortex core radius of superfluid $^4\mathrm{He}(a_0 = 10^{-10}\mathrm{m})$ is much smaller than any of the length scales of interest in turbulent flows. The equation of motion is

$$\dot{\mathbf{s}}(\xi, t) = \mathbf{v}_s + \frac{\beta}{1+\beta} \left[\mathbf{v}_{ns} \cdot \mathbf{s}' \right] \mathbf{s}' + \beta \mathbf{s}' \times \mathbf{v}_{ns} + \beta' \mathbf{s}' \times \left[\mathbf{s}' \times \mathbf{v}_{ns} \right],$$
(8)

where $\dot{\mathbf{s}} = \partial \mathbf{s}/\partial t$, $\mathbf{s}' = \partial \mathbf{s}/\partial \xi$ is the unit tangent vector, $\mathbf{v}_{ns} = \mathbf{v}_n - \mathbf{v}_s$, \mathbf{v}_n and \mathbf{v}_s are the normal fluid and superfluid velocities at \mathbf{s} and β,β' are temperature and Reynolds number dependent mutual fricition coefficients [44]. The superfluid velocity \mathbf{v}_s at a point \mathbf{x} is determined by the Biot-Savart law

$$\mathbf{v}_{s}(\mathbf{x},t) = \frac{\kappa}{4\pi} \oint_{\mathcal{T}} \frac{\mathbf{s}'(\xi,t) \times [\mathbf{x} - \mathbf{s}(\xi,t)]}{|\mathbf{x} - \mathbf{s}(\xi,t)|} d\xi, \qquad (9)$$

where \mathcal{T} represents the entire vortex configuration. There is currently a lack of a well-defined theory of vortex reconnections in superfluid helium, like for the Gross-Pitaevskii equation [42, 43, 57]. An *ad hoc* vortex reconnection algorithm is employed to resolve the collisions of vortex lines [58].

A two-way model is crucial to understand the accurately interept the back-reaction effect of the normal fluid on the vortex line and vice-versa [46]. We self-consistently evolve the normal fluid \mathbf{v}_n with a modified Navier-Stokes equation

$$\frac{\partial \mathbf{v}_n}{\partial t} + (\mathbf{v}_n \cdot \nabla) \mathbf{v}_n = -\nabla \frac{p}{\rho} + \nu_n \nabla^2 \mathbf{v}_n + \frac{\mathbf{F}_{ns}}{\rho_n}, \quad (10)$$

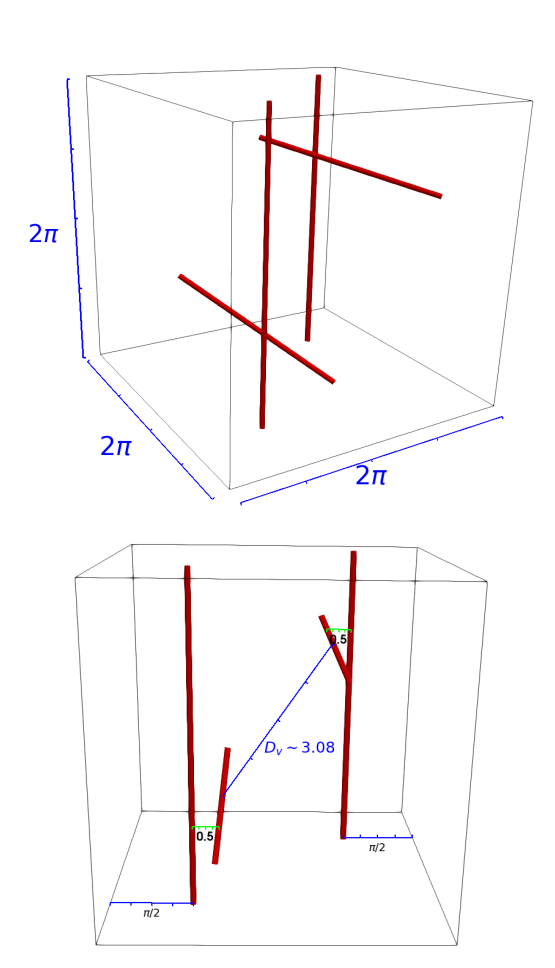


FIG. 5: Schematic diagram of the initial vortex configuration.

$$\mathbf{F}_{ns} = \oint_{\mathcal{T}} \mathbf{f}_{ns} \delta(\mathbf{x} - \mathbf{x}) d\xi, \quad \nabla \cdot \mathbf{v}_n = 0, \quad (11)$$

where $\rho = \rho_n + \rho_s$ is the total density, ρ_n and ρ_s are the normal fluid and superfluid densities, p is the pressure, ν_n is the kinematic viscosity of the normal fluid and \mathbf{f}_{ns}

is the local friction per unit length [59]

$$\mathbf{f}_{ns} = -\mathcal{D}\mathbf{s}' \times [\mathbf{s}' \times (\dot{\mathbf{s}} - \mathbf{v}_n)] - \rho_n \kappa \mathbf{s}' \times (\mathbf{v}_n - \dot{\mathbf{s}}), \quad (12)$$

where \mathcal{D} is a coefficient dependent on the vortex Reynolds number and intrinsic properties of the normal fluid. The regularisation of the mutual fricition force onto the normal fluid grid is physically motivated by the strongly localised injection of vorticity during the momentum exchange of point-like particles and viscous flow in classical fluid dynamics [60, 61]. In short, the localised vorticity induced by the relative motion between the vortex lines and the normal fluid is diffused to discretisation of the grid spacing Δx in a time interval ϵ_R . In this way, the delta-forced fricition as defined in Eq. 12 is regularised by a Gaussian function, the fundamental solution of the diffusion equation. Further details of the method for classical fluids are contained in [60, 61] and for FOUCAULT in [44].

In this Letter, we report all results using dimensionless units, where the characteristic length scale is $\lambda = D/D_0$, where $D^3 = (1 \times 10^{-3} \text{m})^3$ is the dimensional cube size, $D_0^3 = (2\pi)^3$ is the non-dimensional cubic computational domain. The time scale is given by $\tilde{\tau} = \tilde{\lambda}^2 \nu_n^0 \nu_n$, where the non-dimensional viscosity ν_n^0 resolves the small scales of the normal fluid. In these simulations, these quanties are $\tilde{\lambda} = 1.59 \times 10^{-4} \text{m}$, $\nu_n^0 = 0.32$ and $\tilde{\tau} = 0.366 \text{s}$ at T = 1.9K and $\tilde{\tau} = 0.485s$ at T = 2.1K. We consider an initial configuration of two pairs of orthongal vortices, initialised as shown in the schematic of Fig. 5. The separation between vortices in each pair d is set to be $d_v = 0.5$ in dimensionless units, and the shortest distance between pairs is $D_v = \sqrt{(\pi - d_v/2)^2 + \pi^2} \approx 3.08$, so that $d_v \ll D_v$. The Lagrangian discretisation of vortex lines is $\Delta \xi = 0.025$ (a total of 1340 discretisation points across the 4 vortex lines), using a timestep of $\Delta t_{VF} = 5.56 \times 10^{-6}$. For the normal fluid, a total of $N = 256^3$ mesh point were used, with a timestep of $\Delta t_{NS} = 45 \Delta t_{VF}$.